Tunnelling and Underground Space Technology 99 (2020) 103385

Contents lists available at ScienceDirect

Tunnelling and Underground Space Technology

journal homepage: www.elsevier.com/locate/tust

Development of a trench cutting re-mixing deep wall method model test device

Peng Jiang[a,b], Qing-song Zhang[a], Ren-tai Liu[a,*], Adam Bezuijen[b,c], Yan-kai Liu[a], Ke-xian Li[d]

[a] Shandong University, Research Center of Geotechnical and Structural Engineering, 250061 Jinan, China
[b] Ghent University, Department of Civil Engineering, Laboratory of Geotechnics, 9052 Zwijnaarde (Gent), Belgium
[c] Deltares, Geo-engineering, 2600 Delft, the Netherlands
[d] Qingdao Metro Group Corporation, 266000 Qingdao, China

ARTICLE INFO

Keywords:
TRD method
Model test
Uniformity
Sand

ABSTRACT

The trench cutting re-mixing deep wall (TRD) is a new type of underground waterproof curtain. Mixing uniformity is the key index affecting the efficiency and quality of this method. However, because of many influencing factors, existing theories cannot be used to express the relationship between various factors and mixing uniformity. By analyzing the cutting and mixing process of the TRD method, the main factors affecting the uniformity of the mixing were obtained. A model test device was designed and manufactured, based on Buckingham's pi theorem. The validity of the model test device was verified through a comparative analysis of model and field test results. The model test device was demonstrated to be able to simulate the mixing process of the TRD method. The results provide guidance for promotion and better application of the TRD method.

1. Introduction

The trench cutting re-mixing deep wall (TRD) is a new type of underground waterproof curtain. It is only suitable for soft soil layers (sand and peat as well as clay with an undrained shear strength of < 600 kPa) because it uses chain cutters to cut and mix (Peng, 2017). The sand layer is a common water-permeable stratum in a soft soil layer. In the TRD method, the sand layer is forcibly stirred with other layers, destroying its continuity and thereby significantly reducing the permeability of the mixed area. Cement slurry is injected to reduce the permeability further and to increase the strength of the mixed soil. At present, the method has been widely used throughout the world (Garbin et al., 2010, Akagi, 2006, Gularte et al., 2007, Wang et al., 2014). The construction process for this method is shown in Fig. 1.

Mixing uniformity is one of the main purposes of the TRD method, and it is also the key to ensure the treatment effect. If the chain cutters (Fig. 2) cannot move sand particles into other layers and mix with them, it then becomes difficult to retain the subsequently injected cement slurry in the mixed area, which not only seriously affects the treatment effect but also wastes resources. In practice, there have been many incidents of water leakage caused by uneven mixing (Wang, 2017).

Wang, 2017 has conducted much research on the method and given guiding conclusions for various parameters in the application process. With these results, the method was successfully applied in various foundation pit projects. Chaney et al. (2001) and Malusis et al. (2017) have conducted numerous experimental studies on materials used in the TRD method. However, none of the research mentioned above employed model tests on the TRD mixing process. This paper focuses on developing a TRD model test device based on Buckingham's pi theorem, whose rationality was verified by comparing the results of the model and field test. The results showed that the mixing efficiency of TRD reduced when the particle size was large. The sand particles would settle when the diameter of the sand is more than the specific diameter after the mixing procedure stopped.

The model test can replace the field the test which is carried out to measure TRD parameters before construction and has good economics. In addition, the model test device has other benefits. Firstly, the test device can research the mixing time and mixing efficiency of the TRD method, which can reduce costs and improve construction efficiency. Secondly, it can also test the mixing effect of the different shape cutters. Thirdly, the test device can study the difficulty of mixing additional materials with cement soil using the TRD method.

2. Design of the model test device

2.1. Mixing process

During the TRD mixing process, the soil is stripped of the original formation by the cutters, and the clay particles are mixed with the

* Corresponding author.

https://doi.org/10.1016/j.tust.2020.103385
Received 18 June 2019; Received in revised form 9 January 2020; Accepted 8 March 2020

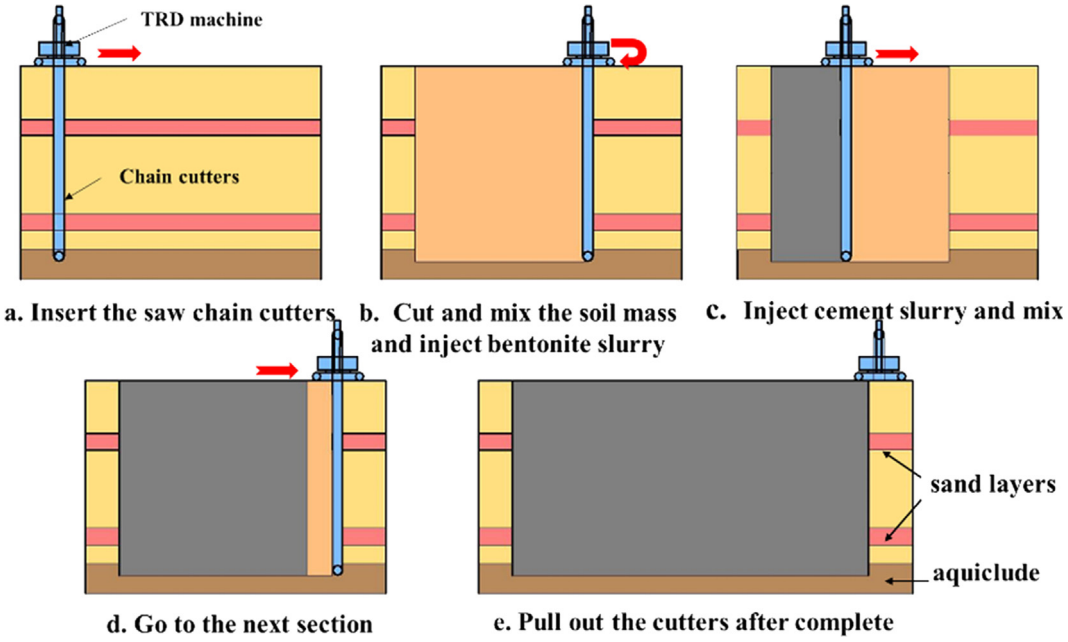

Fig. 1. Schematic diagram showing the steps of the TRD method.

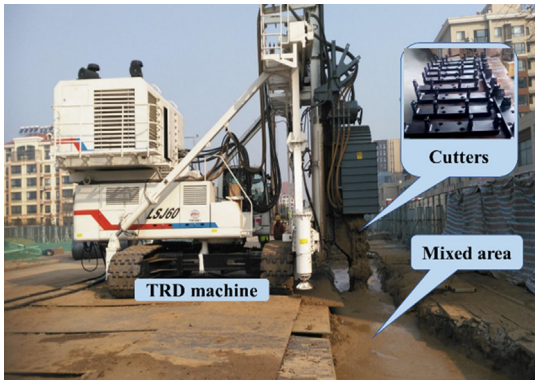

Fig. 2. Photograph of the TRD machine.

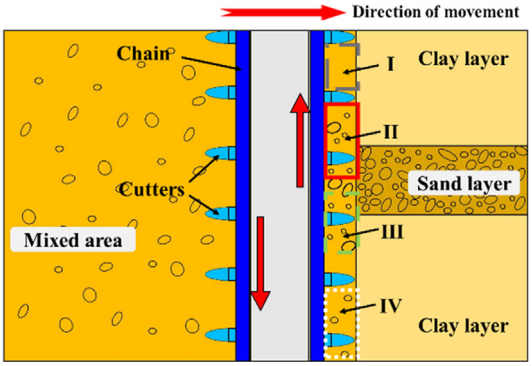

Fig. 3. Schematic diagram of the TRD mixing process.

injected bentonite slurry, as shown in Fig. 3 area I, to form a mixed slurry. Some sand particles from the sand layer are carried upward by the chain cutters, as shown in area II. The other part settles under gravity through the gap between the cutting teeth, as shown in area III, and is mixed with the particles carried by the chain cutters from the bottom of mixing area, as shown in area IV. Then, under the action of the chain cutters, these particles are moved upward and finally mixed with other layers.

To study the influence of the various factors on mixing uniformity, a TRD method model test device was developed. It is based on the excavation project for the Shengliqiao Station exit of Qingdao Metro Line 1 in Qingdao, China, where a field test was conducted to verify the validity of the simulation of the model test device.

2.2. Model test similarity

Similarity is the key to determining the validity of the model test device (Phoon et al., 2019, Wood, 2017). Because there are many factors that influence the mixing process, it is difficult to determine a fixed functional relationship between these factors and mixing uniformity. By analyzing the mixing process, we determined that machine, sand particle, and mixed mud parameters all affect uniformity (Larsson, S., 2005). The machine parameters include the mixing velocity (v), the mixing time (t), and the cutter physical dimension (L). The sand particle parameters include the sand layer depth (H), the grain density (ρ_s), and the grain concentration (C). The mixed mud parameters include the mud density (ρ_f), the mud viscosity (μ), and the mud ultimate shear force (τ_0). From Buckingham's pi theorem (Hassanien et al., 2011), the following function is assumed:

$$f(v, t, L, H, \rho_s, \mu, \tau_0, \rho_f, C) = 0 \tag{1}$$

Taking the cutter physical dimension (L), the mixing time (t), and the grain density (ρ_s) as dimension-independent physical quantities, we have

$$\pi_1 = \frac{v}{t^{\alpha_1} L^{\beta_1} \rho_s^{\gamma_1}} = \frac{L \cdot T^{-1}}{T^{\alpha_1} L^{\beta_1} M^{\gamma_1} \cdot L^{-3\gamma_1}} \tag{2}$$

According to the uniformity of the numerator and the denominator, $\alpha_1 = -1$, $\beta_1 = 1$, and $\gamma_1 = 0$, so

$$\pi_1 = \frac{v_m}{t_m^{-1} L_m} = \frac{v_p}{t_p^{-1} L_p} \tag{3}$$

where the subscript m indicates the model test parameter and the subscript p indicates the in situ parameter.

Furthermore,

$$\pi_2 = \frac{\mu}{t^{-2} L^2 \rho_s} \tag{4}$$

$$\pi_3 = \frac{\tau_0}{t^{-2}L^2\rho_s} \tag{5}$$

$$\pi_4 = \frac{H}{L} \tag{6}$$

$$\pi_5 = \frac{\rho_f}{\rho_s} \tag{7}$$

$$\pi_6 = C \tag{8}$$

where $\pi_1 \sim \pi_6$ are dimensionless parameters.

The model machine cutter was reduced in size from that of the actual cutter, which is large and cannot be applied in the model test, and the ratio is 1/3. The mixing velocity of the model machine was controlled by frequency modulation and was consistent with the in situ stirring velocity. The similarity coefficients of the cutter's physical dimensions (S_L) and the velocity (S_v) are

$$S_L = \frac{L_m}{L_p} = \frac{1}{3} \tag{9}$$

$$S_v = \frac{v_m}{v_p} = 1 \tag{10}$$

Sand and clay encountered in the field tests are also used in the model tests. The soil was compacted during the filling process. After the filling was completed, the density tests were performed to ensure consistency with the field layer. Therefore, the similarity coefficient of the grain density (S_{ρ_s}) is

$$S_{\rho_s} = \frac{\rho_{sm}}{\rho_{sp}} = 1 \tag{11}$$

According to the volume of the soil to be stirred, the amount of cutting fluid was added for cutting and mixing. The model test mixed mud should be the same as the in situ mud. Therefore, the similarity coefficients of the mixed mud viscosity (S_μ), ultimate shear resistance (S_{τ_0}), and density (S_{ρ_f}) are

$$S_\mu = \frac{\mu_m}{\mu_p} = 1 \tag{12}$$

$$S_{\tau_0} = \frac{\tau_{0m}}{\tau_{0p}} = 1 \tag{13}$$

$$S_{\rho_f} = \frac{\rho_{fm}}{\rho_{fp}} = 1 \tag{14}$$

The particle concentration of the model test after mixing was consistent with the in situ value. The concentration similarity coefficient (S_C) is

$$S_C = \frac{C_m}{C_p} = 1 \tag{15}$$

Substituting in each physical quantity gives the sand depth coefficient

$$S_H = \frac{H_m}{H_p} = \frac{1}{3} \tag{16}$$

and the time similarity coefficient

$$S_t = \frac{t_m}{t_p} = \frac{1}{3} \tag{17}$$

The following similarity criteria must be met:

$$\frac{S_v S_t}{S_L} = 1 \tag{18}$$

$$\frac{S_H}{S_L} = 1 \tag{19}$$

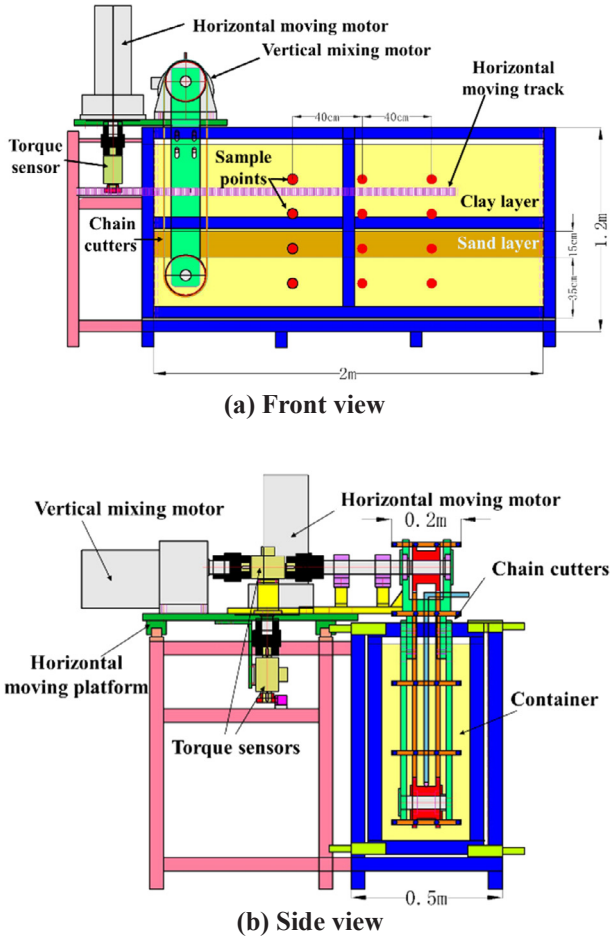

Fig. 4. Schematic diagram of the TRD method model test.

$$\frac{S_\mu S_t^2}{S_L^2 S_{\rho_s}} = 1 \tag{20}$$

$$\frac{S_{\tau_0} S_t^2}{S_L^2 S_{\rho_s}} = 1 \tag{21}$$

$$\frac{S_{\rho_f}}{S_{\rho_s}} = 1 \tag{22}$$

$$S_C = 1 \tag{23}$$

2.3. Model test device

As shown in Figs. 4 and 5, the model test device mainly comprises a vertical mixing device, a horizontal moving device, a grouting device, a container, and a horizontal moving platform. The vertical mixing device is installed on the horizontal moving platform, which is placed on the horizontal track. The horizontal movement and the vertical mixing speed are, respectively, driven by two independent frequency-modulated motors, which are adjusted by two controllers. The horizontal movement speed range is 0–0.1 m/s, and the mixing speed range was 0–1 m/s. Two torque sensors are installed between the motor and the drive gear to monitor the horizontal movement and the mixing load, respectively. Both have a measurement range from 0 to 500 N m. The container has a length of 2 m, a width of 0.5 m, and a height of 1.2 m. The model cutter have a length of 20 cm, a width of 2 cm, and a height of 3 cm, which is one-third of the in situ value.

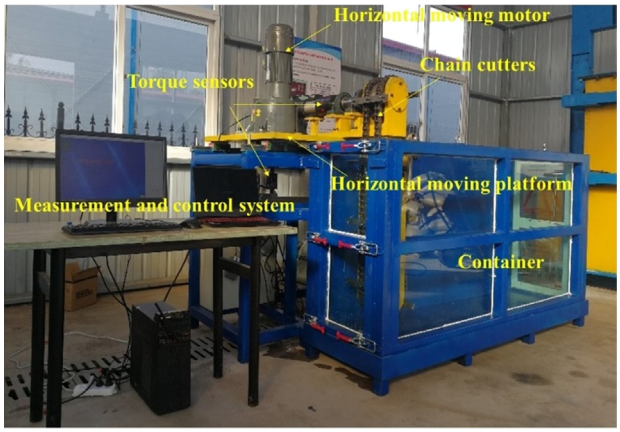

Fig. 5. Model test device.

3. Model tests

The results of the model tests were compared with field test results to verify the validity of the model test device. A 5 m long area was selected as the field test area (Fig. 6) to be simulated in the model; the field test area was taken from the excavation project for the Shengliqiao Station exit of Qingdao Metro Line 1 (Qingdao Geology and Geotechnical Engineering Co., Ltd, 2015).

The thickness of the sand layer in this area is 0.45 m and the mixing depth is 3 m. In the model test, the height of the mixed area was set to 1 m. To meet the sand layer depth coefficient, a 15 cm thick sand layer was filled in the container. A 35 cm clay layer was placed below the sand layer and a 50 cm clay layer was placed above it, as shown in Fig. 4(a). Soil physical parameters were shown in Table 1.

3.1. Sands and soil for model tests

The model test particle volume per sample was equal to that in the field test after mixing evenly, which ensures the correct validation test. The sands and soil for the model test were collected at the time of the excavation of the Shengliqiao Station. The sand particle and soil fill parameters in the model test were consistent with the field tests. The particle-size distribution curve of the sand layer is shown in Fig. 7. The model test sands contained many sand particles with a diameter of > 5 mm.

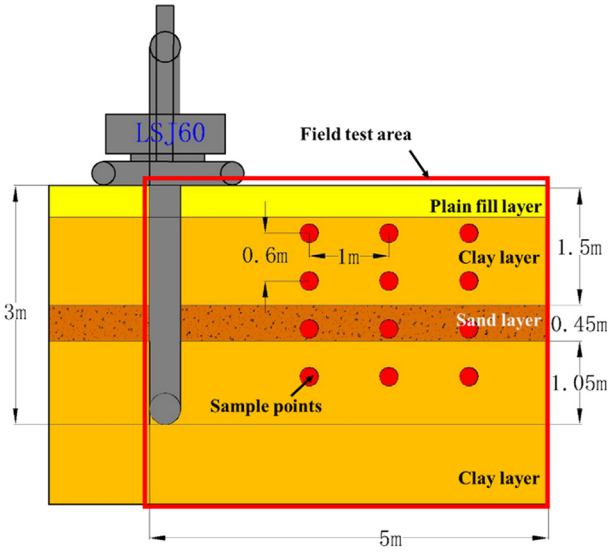

Fig. 6. Stratigraphic profile of the field test area.

3.2. Cutting fluid ratio

The cutting fluid reduces the cutting resistance and increases the moisture content of the mixed area, and it is mixed with the soil particles to form the mixed mud. At the same time, the mixed mud can keep the sand particles suspended to ensure uniformity before solidification. The cutting fluid currently consists of bentonite and tackifiers. The ratios of different soils to bentonite and tackifier are given in Table 2, and the table flow (TF) value of the mixed mud meets the requirements of 180 ± 20 mm (Shi et al., 2013, Ressi and Cavalli, 1985) The mixed area soil was experimentally determined to have 24 kg/m^3 of bentonite. In the model tests, the volume of the soil in the mixed zone was 0.4 m^3. Therefore, 9.6 kg of bentonite was required, and the water/bentonite ratio was 7.5 to meet the TF requirements. In the model test, the cutting fluid was metered by the pump in the mixing area.

3.3. Model test procedure

The mixing device was moved to one end of the container. The sands and soil were filled into the tank, and the layer was compacted step by step to ensure similarity to the field layer. In each layer, a cutting ring is used to take samples to test the density and moisture of the filled soil, which could ensure that the soil in the model test is consistent with the in-situ soil. After the completion of the filling, as shown in Fig. 8, the vertical mixing motor was turned on, and the corresponding bentonite slurry was injected uniformly at the end of the chain cutters. The vertical mixing speed was adjusted after the device ran smoothly. The horizontal moving motor was turned on and adjusted to the required horizontal moving speed. When the cutting device entered the particle collection point (Fig. 4), the sample collection device (Fig. 9) was used to collect the sample, the volume of which was 25 ml. Sands in the sample with diameters of > 0.5 mm were weighed after cleaning and sieving. Particle concentrations measured at the same sampling point depth were arithmetically averaged to obtain this particle concentration of this depth.

3.4. Model test contents

Four groups of tests (Table 3) were conducted with different diameters of sand particles: in situ sands and sands with diameters of 2–5, 5–7.5 (Fig. 8), and 10–15 mm (see Table 4).

4. Field test

The field test (see Fig. 10) was conducted by using an LSJ60 machine (see Fig. 2) from China Railway Construction Heavy Industry Co. Ltd., as shown in Fig. 11. The mixing speed was 1 m/s, and the horizontal moving speed was 2 m/h, which are consistent with the running speeds of the model test machine.

Fig. 6(a) shows the sampling points. They are consistent with the layout of the model test sampling points, and the same sampling method was used in the field test. The sampling points had a horizontal spacing of 1 m, being located at horizontal positions of 2, 3, and 4 m, and a vertical spacing of 0.6 m, respectively, at four locations of 0.6, 1.2, 1.8, and 2.4 m, for a total of 12 sampling points. The results of the field test were treated in the same way as those of the model test.

5. Analysis of test results

5.1. Model test results

(1) The first group of tests was conducted using sand from the Shengliqiao Station. The test results are shown in Fig. 11.

After the beginning of the test, the sand concentration became more uniform. The sand concentration was close to a uniform state after 90s,

Table 1
Soil physical parameters of field test.

No	Depth (m)	Soil density (g/cm^3)	Grain density (g/cm^3)	Liquid limit (%)	Plastic limit (%)	Moisture(%)	Cohesive strength (kPa)	Internal friction angle (°)
1	0.7	1.97	2.74	37.2	19.8	27.5	31.3	10.2
2	1.0	2.08	2.74	37.2	19.8	24.5	38.3	8.8
3	1.3	2.01	2.74	37.3	19.7	25.0	35.2	11.3
4	2.2	1.98	2.75	37.4	17.7	25.3	22.3	10.3
5	2.5	2.01	2.75	37	17.8	23.8	28.5	18.1

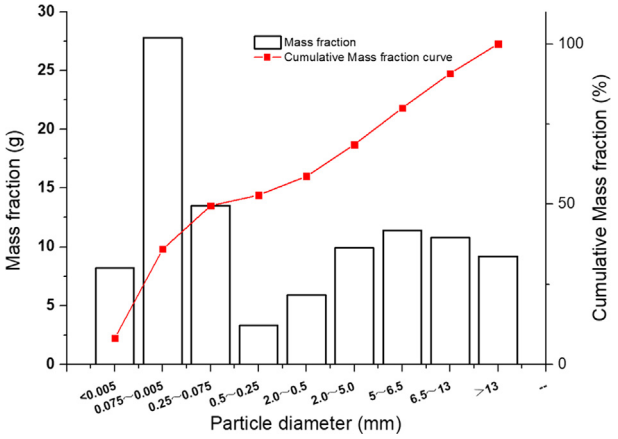

Fig. 7. Particle-size distribution curve of the model test sands.

Table 2
Mixing ratios of cutting fluid (per 1 m^3 of undisturbed soil).

Soil conditions	Additive	
	Bentonite (kg)	Tackifier (kg)
Clayey soil	0–5	0
Fine sand	5–15	0
Medium sand, coarse sand	15–25(20)	0–1
Gravel sand, gravel	25–50(30)	0–2.5
Cobblestone, crushed stone	50–75(40)	0–5.0

Fig. 8. Photograph of the filled container.

and the rate of change then lessened. The particle diameter of the sand was < 10 mm; the sand particles were collected at sampling points of 20 and 40 cm in depth during this time. As mixing continued, larger particles appeared, and the particle concentration slowly increased to a uniform level, but the mixing efficiency decreased significantly. After mixing began, the sand particles of the 60 cm depth collapsed into the 80 cm depth sampling point, thus causing a drastic change at the 60 and 80 cm deep sampling points. After mixing for 210 s, the particle concentration no longer changed. The mixing was stopped at 240 s. The particle concentration decreased at depths of 20 and 40 cm, and the particle concentration at the 80 cm depth increased, which was caused by the free sedimentation of the larger sand particles.

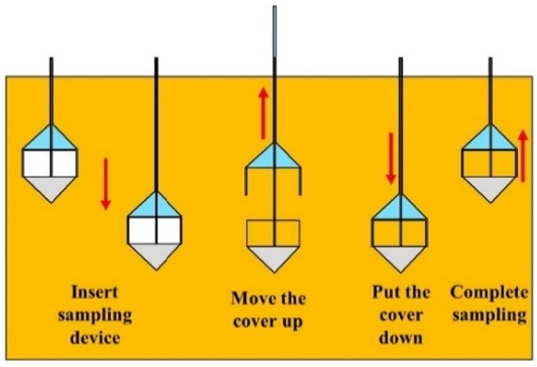

Fig. 9. Schematic diagram of the sand particle collection device.

Table 3
Model test contents.

Test No	Diameter of sand (mm)	Depth (cm)	Thickness (cm)
1	2–5	50–65	15
2	5–7.5		
3	10–15		
4	in situ sands		

Table 4
Comparison of permeability before and after mixing in the field test.

No	Layer	Depth (m)	Permeability (cm/s)	
			Before mixing	After mixing
1	Plain fill	0.2	7.2×10^{-2}	3.2×10^{-7}
2	Clay	0.8	3.8×10^{-5}	2.8×10^{-7}
3	Sand	1.7	5.2×10^{-2}	2.5×10^{-7}
4	Clay	2.5	1.5×10^{-6}	4.7×10^{-7}

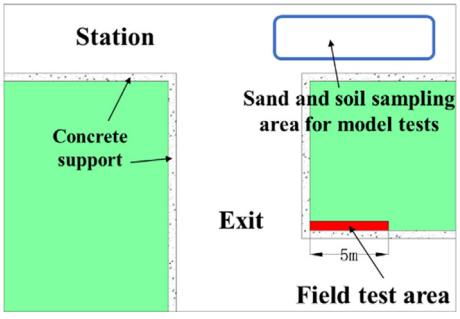

Fig. 10. Field test area plan.

(2) From the theory of solid–liquid two-phase flow (Nunziato, 1983), it is known that sand particles have a specific particle diameter in a clay slurry, and sand particles of this diameter are just suspended in the mixed mud. The specific particle diameter is determined by the particle density and the properties of the mixed mud. Through the above test, it was found that particles with diameters of > 10 mm

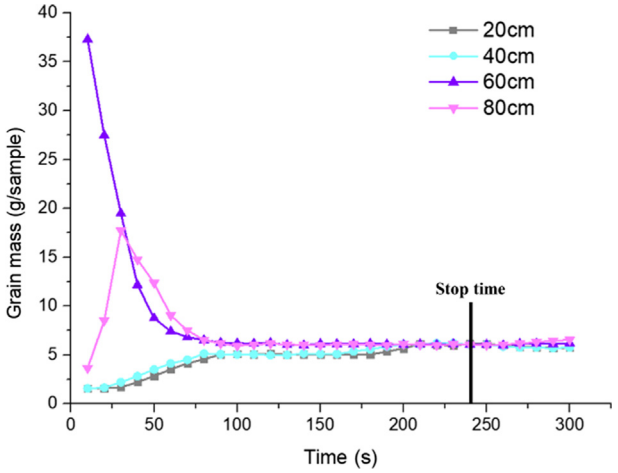

Fig. 11. Concentration curves of the Shengliqiao station particle with time in the model test.

precipitated, and the efficiency of uniform mixing decreased. Therefore, 10 mm is the special particle diameter. Three sets of simulation tests with particle diameters of 2–5, 5–7.5, and 10–15 mm were performed, with other test parameters remaining unchanged.

As shown in Figs. 11 and 12, the shape of the particle concentration changes with time in the same manner in the four simulation tests, and sand particles of different diameters can be evenly distributed in the mixed mud. A comparison of the results of the three different diameter particles shows that the 2–5 and 5–7.5 mm particles were suspended in the mixed mud, and no sedimentation occurred after mixing stopped. As shown in Fig. 12(c), the concentration curves of 10–15 mm particles changed drastically, and the mixing time was increased to 840 s. After the mixing stopped, particle sedimentation occurred at the 20 cm and 40 cm depths and particle deposition occurred at the 80 cm depth. The front and side plates of the model test container were opened for sampling after the mixed mud solidified, and the deposition area (60 cm to 80 cm in depth) is shown in Fig. 13.

Therefore, if the particle diameter is smaller than the specific particle diameter, the sand layer is easily mixed uniformly at the depth about 50 cm (Fig. 14). When the mixing stops, no sedimentation occurred. When the particle diameter is larger than the specific particle diameter, the sand layer is difficult to be evenly mixed, and the mixing efficiency is low. Both upper particle sedimentation and lower particle accumulation are likely to occur.

As shown in Fig. 15, the results of four simulation tests indicate that sand particles with different diameters have little effect on the torque under the same parameters.

5.2. Field test results

By analyzing the simulation and field test results (Figs. 11 and 16), one can conclude that the curves of particle concentration over time in the two tests are approximately the same. The uniform mixing time in the field test was 640 s, which is a factor of 3.05 greater than that of the model tests. The result is approximately the same as for the time similarity coefficient of the model test design. Therefore, the model test device can simulate the TRD mixing process.

Mixing was stopped at 690 s, and a certain amount of particle concentration sedimentation occurred at the 0.6 m and 1.2 m sampling points, which was consistent with the model test phenomenon. By sieving, it was found that the sinking particles were mainly particles having a diameter of > 10 mm. Therefore, the cement slurry should be injected in time to prevent a large number of particles from settling, which ensures the mixing effect.

As shown in Fig. 17, the particle-size distribution curve after

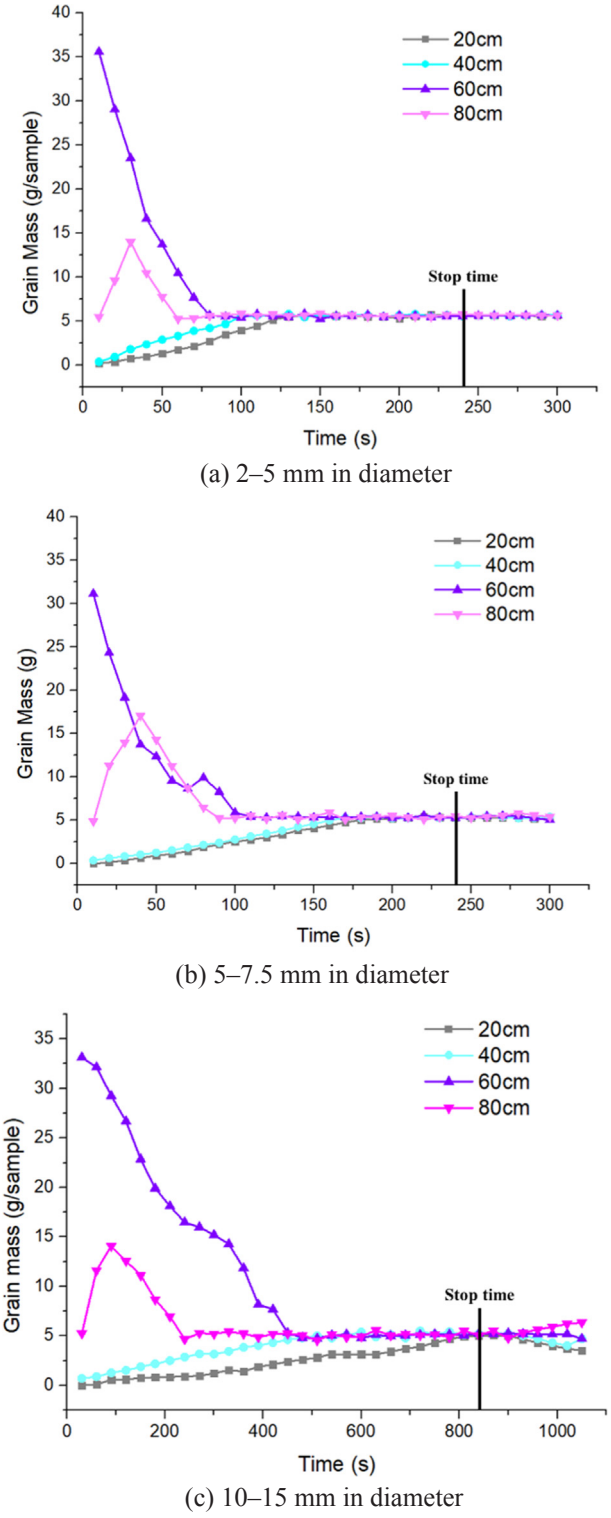

Fig. 12. Concentration curves of different diameter particles with time in the–model test.

uniform mixing was significantly improved. Because the medium coarse sand layer was mixed and evenly distributed in the stirring area, the content of particles having diameters of > 5 mm was lowered. After 28 days of injecting the cement slurry, it was found that the particles were evenly distributed in the core samples obtained by drilling, as shown in Fig. 18. At the same time, the permeability was measured, and reached 2.5×10^{-7} cm/s, which met the design requirements (Shi et al., 2013). The method applies to the middle coarse sand layer in the

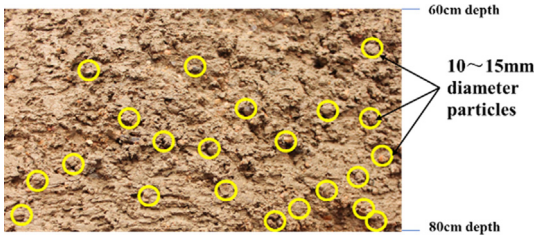

Fig. 13. 10–15 mm diameter particles deposition area in model test.

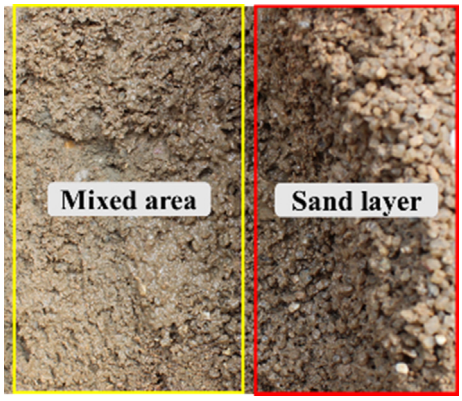

Fig. 14. Comparison of 2–5 mm diameter sand layers after solidification.

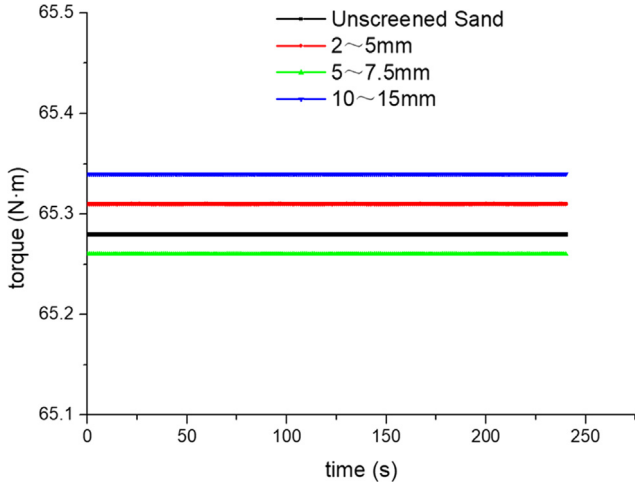

Fig. 15. Torque curves during mixing.

Qingdao area.

6. Conclusions

Through the model and field tests, the following conclusions are obtained:

(1) The uniform mixing time in the field test was 640 s, which is a factor of 3.05 greater than that of the model tests. The result is approximately the same as for the time similarity coefficient of the model test design. Therefore, the model test device can simulate the TRD mixing process.

(2) The single sand layer particle concentration mixing curve was obtained. In the upper part of the sand layer, the particle concentration slowly increases to a uniform level. The particle concentration in the sand layer decreases rapidly. In the lower portion of the sand layer, the particle concentration first increases quickly because of sand layer caving and then slowly drops.

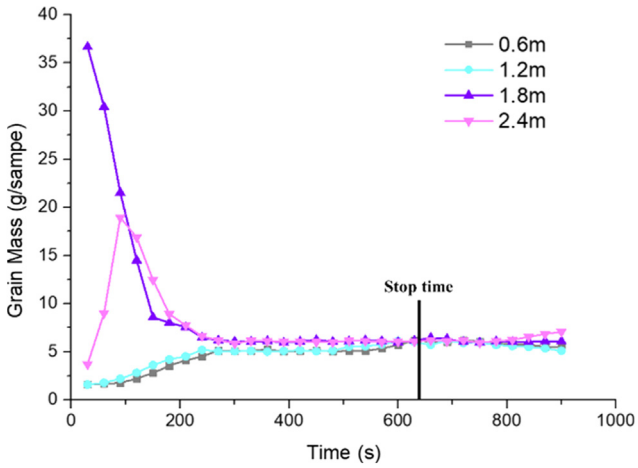

Fig. 16. Concentration curves of > 5 mm particles with time in the field test.

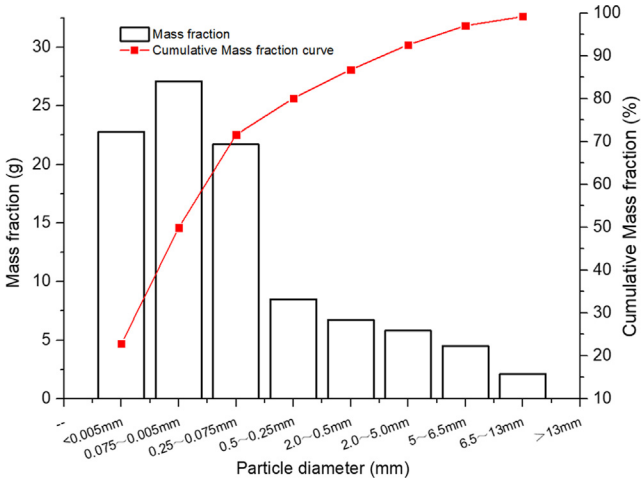

Fig. 17. Particle-size distribution curve of the mixed area.

Fig. 18. Photograph of the core sample at 2 m depth in the field test area.

(3) Under the same conditions, when the diameter of sand particles is > 10 mm, the time for even mixing increases notably, which affects the stirring efficiency.10 mm is the specific particle diameter for the Shengliqiao Station. The different diameter particles have less influence on the torque than during the stirring process.

(4) If the particle diameter is smaller than the specific particle diameter, the sand layer is easily mixed uniformly and no sedimentation occurred after stopping the mixing. When the particle diameter is larger, the sand layer is difficult to be evenly mixed and the mixing efficiency is low. Both upper particle sedimentation and

lower particle accumulation are likely to occur.

The model test device will enable studies of how new soil stabilizer materials and the cutting fluid influence the performance of the mixed wall during the mixing process in the future. Moreover, the relationship between the mixing parameters can be further researched.

CRediT authorship contribution statement

Peng Jiang: Conceptualization, Formal analysis, Writing - original draft, Validation, Data curation. **Qing-song Zhang:** Resources, Supervision, Funding acquisition. **Ren-tai Liu:** Methodology, Writing - review & editing, Project administration. **Adam Bezuijen:** Writing - review & editing. **Yan-kai Liu:** Investigation, Data curation. **Ke-xian Li:** Investigation, Supervision.

Declaration of Competing Interest

The authors declare that they have no known competing financial interests or personal relationships that could have appeared to influence the work reported in this paper.

Acknowledgements

The project is funded by the Qingdao Metro Group Corporation, the Joint Funds of the National Natural Science Foundation of China under Grant No. U1706223, and the General Program of the National Natural Science Foundation of China under Grant No. 51879152. Thanks are owed to the China Scholarship Council and Professor Adam Bezuijen for providing opportunities to study at Ghent University.

Appendix A. Supplementary material

Supplementary data to this article can be found online at https://doi.org/10.1016/j.tust.2020.103385.

References

Akagi, H., Kondo, Y., Nakayama, T., Naoe, H., 2006. Cost Reduction of Diaphragm Wall Excavation Using Air Form and Case Record, 15th ICEG Environmental Geotechnics. Thomas Telford, London, pp. 685–692.

Chaney, R. C., K. R. Demars, S. Lee, and I. Lee, Retaining Wall Model Test with Waste Foundry Sand Mixture Backfill, Geotechnical Testing Journal 24, no. 4(2001), pp. 401–408.

Garbin, E., Hussin, J., Kami, C., 2010. Earth Retention Using the TRD Method, Earth Retention Conference (ER), Bellevue, Washington, pp. 318–325.

Gularte, F., Barneich, J., Burton, J., Fordham, E., Wat, D., Johnson, T., Weeks, J., 2007. First Use of TRD Construction Technique for Soil Mix Cutoff Wall Construction in the United States. Denver, GeoDenver, pp. 12.

Hassanien, I. A., Salama, A.A., Hosham, H. A., 2011. Analytical and Numerical Solutions of Generalized Burgers Equation Via Buckingham's Pi-theorem. Can. J. Phys. 83, 10 (2011), 1035–1049.

S. Larsson, State of practice report – Execution, monitoring and quality control, Proceedings of the International Conference On Deep Mixing – Best Practice and Recent Advances, vol. 2, (2005), pp.732–785.

Malusis, M. A., Evans, J. C., Jacob, R. W., Marchiori, A. M., 2017. Construction and Monitoring of an Instrumented Soil–Bentonite Cutoff Wall: Field Research Case Study, Central Pennsylvania Geotechnical Conference, Hershey.

Nunziato, J.W., 1983. A Multiphase Mixture Theory for Fluid–particle Flows, Theory of Dispersed Multiphase Flow. New York: Academic, (1983).

Peng, Y., 2017. Development Course and Prospect of the Chain Cutter Type of Underground Diaphragm Wall Equipment, Construction Technology, Beijing, 46, no. 22(2017), pp. 124–128.

Phoon, K.-K., Tang, C., 2019. Characterisation of Geotechnical Model Uncertainty, Georisk Assessment and Management of Risk for Engineered Systems and Geohazards, 13, 6(2019), 1–30.

Qingdao Geology and Geotechnical Engineering Co., Ltd. Geotechnical Investigation Report of Shengliqiao Station of Qingdao Metro Line 1 (in china), Qingdao: Qingdao Geology and Geotechnical Engineering Co., Ltd., (2015).

Ressi, A., Cavalli, N., 1985. Bentonite Slurry Trenches, Engineering Geology, Amsterdam, pp. 333–339.

Shi, Z.Y., Liu, X.W., Gong, X.N., Fan, L.B., 2013. Technical Specification for Trench Cutting Re-mixing Deep Wall (in china). Ministry of housing and urban-rural development of the People's Republic of China.

Wang, W.D., 2017. Technology and Practice of Uniformly Thick Cement Soil Mixing Wall (in china). China Architecture & Building Press, Beijing.

Wang, W.-D., Q.-P. Weng, Chen, Y.-C., 2014. Experimental Investigation of Construction of a 56 m Deep Constant Thickness Cement–soil Wall Using Trench Cutting Re-mixing Deep Wall (TRD) Method in Deep Aquifers, Rock and Soil Mechanics 35, no. 11(2014), pp. 3247–3252.

Wood, D.M., 2017. Geotechnical Modelling, London and New York: Spon Press. (2017).